51-YEAR WAVE HINDCAST AND ANALYSIS OF WAVE HEIGHT CLIMATE TREND ON THE NORTHWESTERN PACIFIC OCEAN

M. Yamaguchi and Y. Hatada

Department of Civil and Environmental Engineering , Ehime University
Matsuyama, Ehime Prefecture, Japan

1. INTRODUCTION

Since long-term variability of wave climate, specifically an increasing trend of wave height related to environmental change probably due to global warming may enhance the potential for wave-induced coastal disasters and have a bad influence on the the safety of maritime structures, elucidating the real state is of great concern for not only scientists but also engineers. In the recent 15 years, variability of wave climate on the North Atlantic Ocean has been extensively investigated using measurement data (Carter and Draper, 1988) and hindcast data over long years (Bacon and Carter, 1991; Kushnir et al., 1997; Gunther et al., 1998). Also, wave climate on the global scale is discussed by Suzuki et al. (1996) and Sterl and Komen (1998) using hindcast data over 15 years, in cases in which a year period of wave hindcast may be too short to investigate variability of wave climate. Recently, Cox and Swail (2001) has conducted wave hindcasting on the global scale over the 40 years from 1958 to 1997 and trend analysis of wave height, in cases where the input wind data is extracted from the 6-hourly NCEP/NCAR (National Centers for Environmental Prediction/National Center for Atmospheric Research) reanalysis surface wind data archive. But relatively low space resolution in wave hindcast of 1.25 degrees in latitude by 2.5 degrees in longitude may make it unsatisfactory to investigate wave climate and its trend in the marginal sea areas such as sea areas around Japan.

The NCEP/NCAR reanalysis surface wind data sets over the 51 years from 1948 to 1998 on the global scale are now opened to the public domain. The aim of the study is to hindcast waves at 52 properly-selected points on the Northwestern Pacific Ocean location by location every 1 hour over 51 years by applying a shallow water model with use of a backward ray tracing method on a grid with 5 km space resolution under the NCEP/NCAR reanalysis wind condition and to investigate increasing or decreasing trend of wave climate parameters on the area based on the analysis of long-term hindcast data after validation of the wave model on the basis of the comparison between hindcasts and measurements at 4 buoy stations in the recent 10 years.

2. DESCRIPTION OF THE METHODOLOGY

2.1 *NCEP/NCAR Wind Data Set*

The 6-hourly wind data at 10 m height over the 51-year period from 1948 to 1998 is gathered from the NCEP/NCAR reanalysis surface wind data sets provided by NCAR, which is referred to as NCEP/NCAR wind data hereafter. The original NCEP/NCAR wind data is given on a Gaussian grid with space resolution of about 1.9 degrees. For use in wave hindcast, the NCEP/NCAR wind data is remade through a spatial interpolation onto the Cartesian grid with a spacing of 80 km on the Northwestern Pacific Ocean area and consequent one-hourly linear interpolation with time.

2.2 *Wave Model and Conditions of Wave Hindcast*

A shallow water wave model based on backward ray tracing (Yamaguchi et al., 1987) is used for long-term wave hindcasting. The model follows the change of directional spectrum along a refracted ray of each component wave focusing on a hindcast point. The wave ray is traced on the Northwestern Pacific Ocean area divided into 673 by 673 with a grid size of 5 km, where the grid has a rather high space resolution. Wind components are bi-linearly interpolated onto a wave ray of each component using the one-hourly NCEP/NCAR wind data on a regular grid. The number of frequency data used in wave hindcasting is 23 ranging from 0.04 to 0.5 Hz and the number of direction data is 36 equally divided on the whole circle. The directional spectrum

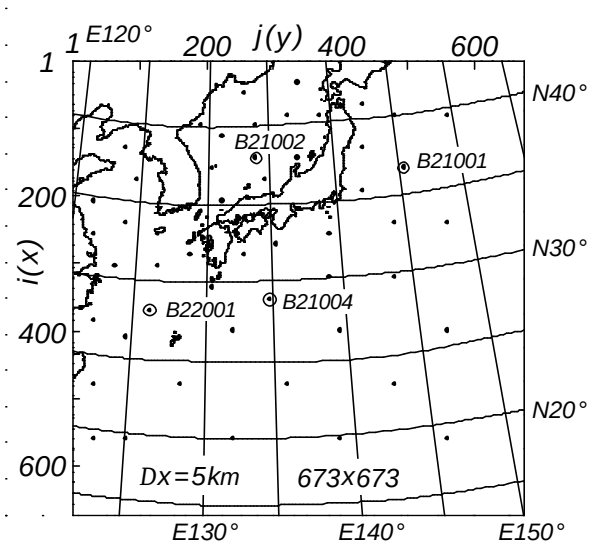

Figure 1. Computation area on the Northwestern Pacific Ocean and location of 52 wave hindcast points including 4 buoy stations.

parameterized with local wind speed and direction is prescribed at the tip of each ray reaching the open boundary and the condition of zero directional spectrum is given at the land boundary.

The model computes one-hourly variation of directional spectrum and the resulting significant waves with mean wave direction at a hindcast point over the 51-year period from 1948 to 1998. The wave hindcasting is conducted at each of 52 points including 4 buoy stations distributed so as to cover the Northwestern Pacific Ocean, as is shown in Figure 1. The points near open sea boundary are located about 700 km inside from the boundary in order to keep fetches for wave growth. The model is a decoupled propagation model belonging to the first generation, but the accuracy compares favorably with WAM at the level of significant waves (Hatada et al., 2000).

As be mentioned below, the NCEP/NCAR wind data tends to yield lower wind speed than actual one for higher wind conditions because of its poor space-time resolution and consequently the same feature appears in the hindcast wave data. For the purpose of dealing with the problem by a convenient way, a coefficient in the wave growth term is tuned so as to give greater growth for higher wind speed compared to the original wave model.

2.3 *Methods of Data Analysis*

Using the time series of hindcast and measured wave height data, various kinds of wave height climate parameters and error statistics are calculated for a whole year period and separately for each year and month on a whole year period. The wave height climate parameters are the mean and standard deviation of significant wave height (SWH) data $\overline{H}$, H_s , the highest 1/3 mean of SWH data $H_{1/3}$ and the highest 1/10 mean of SWH data $H_{1/10}$. Also, the error statistics are the correlation coefficient between hindcasts and measurements for wave height ? $_H$, the slope value of a straight line passing through the origin in the correlation diagram between hindcasts and measurements a_{0H}, and the root mean square error (RMSE) of wave height s $_H$. The trend analysis for year-grouped wave height climate parameters is made in two ways. One is to fit a straight line to time series of the wave climate parameters, such that

$$\overline{H} = a(\overline{H})*t + b(\overline{H}) \tag{1}$$

where t is the year. Slope value $a(\overline{H})$ and intersection value $b(\overline{H})$ are determined by the least square method. The slope value $a(\overline{H})$ is used to see an increasing or decreasing linear trend in the time series according to the

sign. The other is to make use of the trend index I_T introduced by Suzuki(1975). For the time series with a sample size of more than 20, the criterion at a confidence level of 95 % is as follows.

$|I_T|<1.65$: no trend
$I_T> 1.65$: increasing trend, $I_T<-1.65$: decreasing trend (2)

The same methods are also applied for the analyses of wind speed climate parameters and their trends using the NCEP/NCAR wind data, in cases where direction-grouped occurrence rates of all wind speed data and high wind speed data greater than 10 m/s over a whole measurement year period are added.

3. VALIDATION OF NCEP/NCAR WIND DATA AND HINDCAST WAVE DATA

3.1 *Comparison with Measured Wind Data*

Assuming that wind data at 4 buoy stations deployed by Japan Meteorological Agency are not assimilated into the NCEP/NCAR wind data, comparison between reanalysis and measurement data is continued. Figure 2 indicates contour plot of relative occurrence frequency between reanalysis and measurement for 6-hourly wind speed over the whole measurement year periods at 4 buoy stations. As was shown in Figure 1, name of the buoy stations are B21001 located on the sea area east of north Japan, B21002 on the central part of the Japan Sea, B21004 on sea area south of west Japan and B22001 on the East China Sea. Table 1 also lists the wind climate parameters based on reanalysis and measurement data over an entire measurement period such as mean and standard deviation of wind speed data ($\overline{U}$, U_s), and the wind speed error statistics consisting of correlation coefficient ? $_U$, slope value a_{0U} and RMSE of wind speed s $_U$, in which measurement rate r_U and measurement year period are also given. At B21001 station with several tens of kilometers of change of the deployment position before and after 1987 and withdrawal in 1991, the measurement year period of 8 years from 1983 to 1990 is shorter and the measurement rate of 0.661 is lower, compared to the measurement year period of 10 years from 1989 to 1998 and the measurement rates from 0.931 to 0.980 at the other 3 buoy stations.

At 3 stations except for B21001, relatively high correlation between reanalysis and measurement data is suggested by contourlines with slender elliptic forms, while at B21001, lower correlation is indicated by

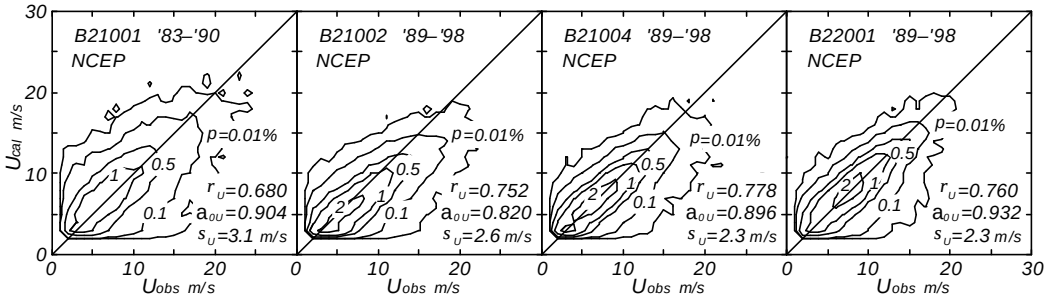

Figure 2 . Contour plot of relative occurrence frequency between reanalysis and measurement for 6-hourly wind speed at 4 buoy stations.

Table 1. Wind speed climate parameters based on reanalysis and measurement data and error statistics.

Buoy	$\overline{U}_{\text{cal}}$	$\overline{U}_{\text{obs}}$	$U_{s\ \text{cal}}$	$U_{s\ \text{obs}}$	? $_U$	a_{0U}	s $_U$	r_U	year period
B21001	7.3	7.3	3.5	4.1	0.680	0.904	3.1	0.661	1983~ 1990
B21002	6.0	6.7	3.0	3.8	0.752	0.820	2.6	0.961	1989~ 1998
B21004	6.3	6.5	2.9	3.6	0.778	0.896	2.3	0.980	1989~ 1998
B22001	7.1	7.1	3.1	3.5	0.760	0.932	2.3	0.939	1989~ 1998

$\overline{U}_{\text{cal}}$, $\overline{U}_{\text{obs}}$, $U_{s\ \text{cal}}$, $U_{s\ \text{obs}}$, s $_U$: m/s

contourlines with flat elliptic forms. Also, the NCEP/NCAR wind data tends to give weaker wind speed than the measurement data for stronger wind speed cases, a feature which is clearly seen at B21002. As for the mean wind speed $\overline{U}$, close agreement between reanalysis and measurement data is found except for B21002. But the wind speed climate parameter U_s and the 3 error statistics ? $_U$, a_{0U}, s $_U$ suggest the above-mentioned tendency.

Figure 3 shows comparison of monthly-grouped wind speed climate parameters based on reanalysis and measurement data at 4 buoy stations. As for the mean wind speed $\overline{U}$, reanalysis data yields reasonable agreement with measurement data except for B21002, but as for the parameters representing higher wind parts such as $U_{1/3}$ and $U_{1/10}$, reanalysis data gives increasingly lower values than measurement data in turnof $U_{1/3}$ and $U_{1/10}$, as is indicated by correlation coefficient and slope value in each figure. This is the reason that a coefficient of growth term in the wave model is changed to obtain better estimates for higher waves.

Direction-grouped occurrence rates of both all wind speed data and high wind speed data greater than 10 m/s are compared in Figure 4. Overall agreement is observed at any of the buoy stations, although occurrence of the N direction component in reanalysis data is less than that in measurement data at B21001 and B21002. It should be noted that strong winds on the Northwestern Pacific Ocean are likely to blow from a range of north to northwest, where fetch-limited waves may be predominant, being associated with the upwind directions bounded by the continent and Japan Islands.

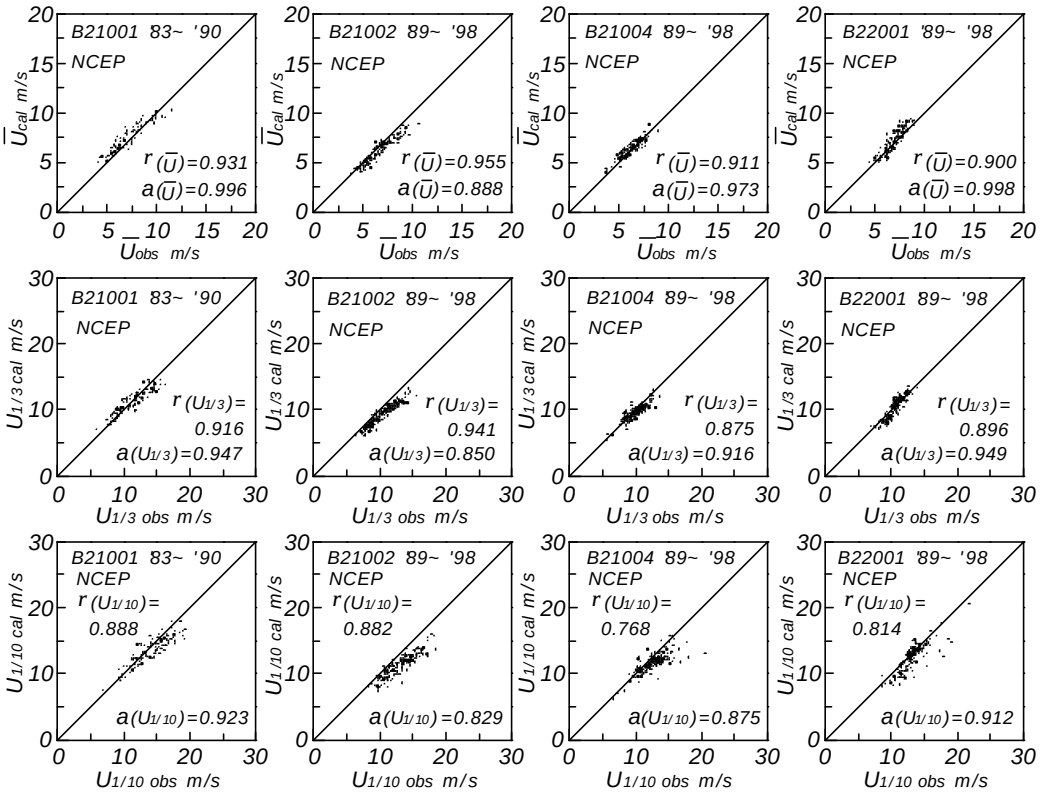

Figure 3. Comparison of monthly-grouped wind speed climate parameters based on reanalysis and measurement data at 4 buoy locations.

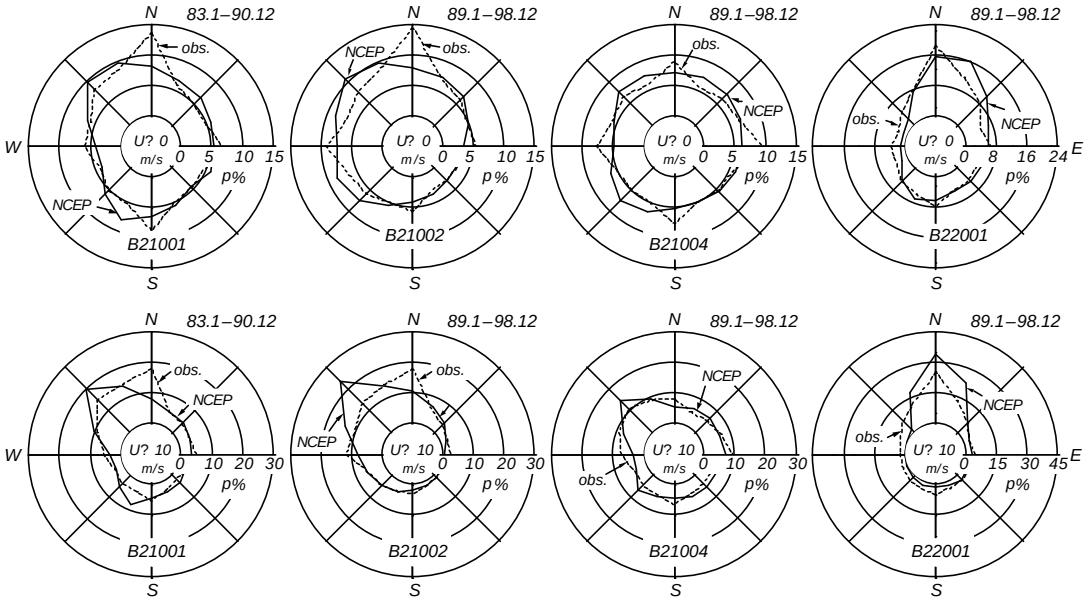

Figure 4. Comparison of direction-grouped occurrence rates of all wind speed data and high wind speed data at 4 buoy stations.

3.2 *Comparison with Measured Wave Data*

Data of SWH before August 1, 1990 at buoy stations are obtained from mean value of 20-individual wave height multiplied by 1.60, while data of SWH after August 1, 1990, is made directly from the measured record. This means lower statistical reliability of the data before August 1, 1990. Figure 5 describes contour plot of relative occurrence frequency between hindcast and measurement for 3-hourly wave height at 4 buoy stations and Table 2 summarizes the wave height climate parameters based on hindcast and measurement over a whole measurement period and their error statistics with measurement rate r_H and measurement year period. It is noted that the measurement rate for waves is not so high as that for winds at any of the buoy stations. Generally, reasonable agreement between hindcast and measurement is found at each of 4 buoy stations. In a more detailed aspect, contourlines with flat elliptic form at B21001 suggest lower correlation compared to the other stations, and hindcast at B21004 becomes smaller than measurement for higher wave conditions. These reflect features of the NCEP/NCAR wind data. The wave height climate parameters based on hindcast and measurement data and the error statistics in the table suggest the above-mentioned tendencies.

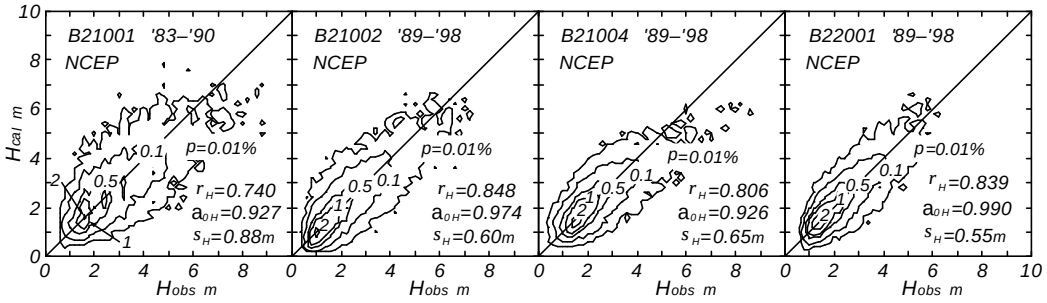

Figure 5. Contour plot of relative occurrence frequency between hindcast and measurement for 3-hourly wave height at 4 buoy stations.

Table 2. Wave height climate parameters based on hindcast and measurement and error statistics.

Buoy	$\overline{H}_{cal}$	$\overline{H}_{obs}$	$H_{s\ cal}$	$H_{s\ obs}$	? $_H$	a_{0H}	s $_H$	r_H	year period
B21001	2.37	2.35	1.13	1.28	0.740	0.927	0.88	0.581	1983~ 1990
B21002	1.79	1.77	1.09	1.06	0.848	0.974	0.60	0.582	1989~ 1998
B21004	1.99	1.98	0.91	1.09	0.806	0.926	0.65	0.694	1989~ 1998
B22001	1.91	1.84	0.95	0.98	0.839	0.990	0.55	0.729	1989~ 1998

$\overline{H}_{cal}$, $\overline{H}_{obs}$, $H_{s\ cal}$, $H_{s\ obs}$, s $_H$: m

Comparison of monthly-grouped wave height climate parameters based on hindcast and measurement is shown in Figure 6. As for the mean SWH $\overline{H}$ and the highest 1/3 mean SWH $H_{1/3}$, a rather high correlation between hindcast and measurement is observed on the whole, but as for the highest 1/10 mean SWH $H_{1/10}$, the hindcast gives lower values compared to the measurement. This result indicates that enhancing growth rate in the wave model is successful for wave estimation to some degree, but that it is still not satisfactory for higher waves.

Figure 7 describes interannual variations of yearly-grouped wave height climate parameters estimated using hindcast and measurement data, and measurement rate.The hindcast yields relatively good agreement with the measurement for $\overline{H}$ and $H_{1/3}$, while the correspondence for $H_{1/10}$ is specifically poor at B21004. It can be said

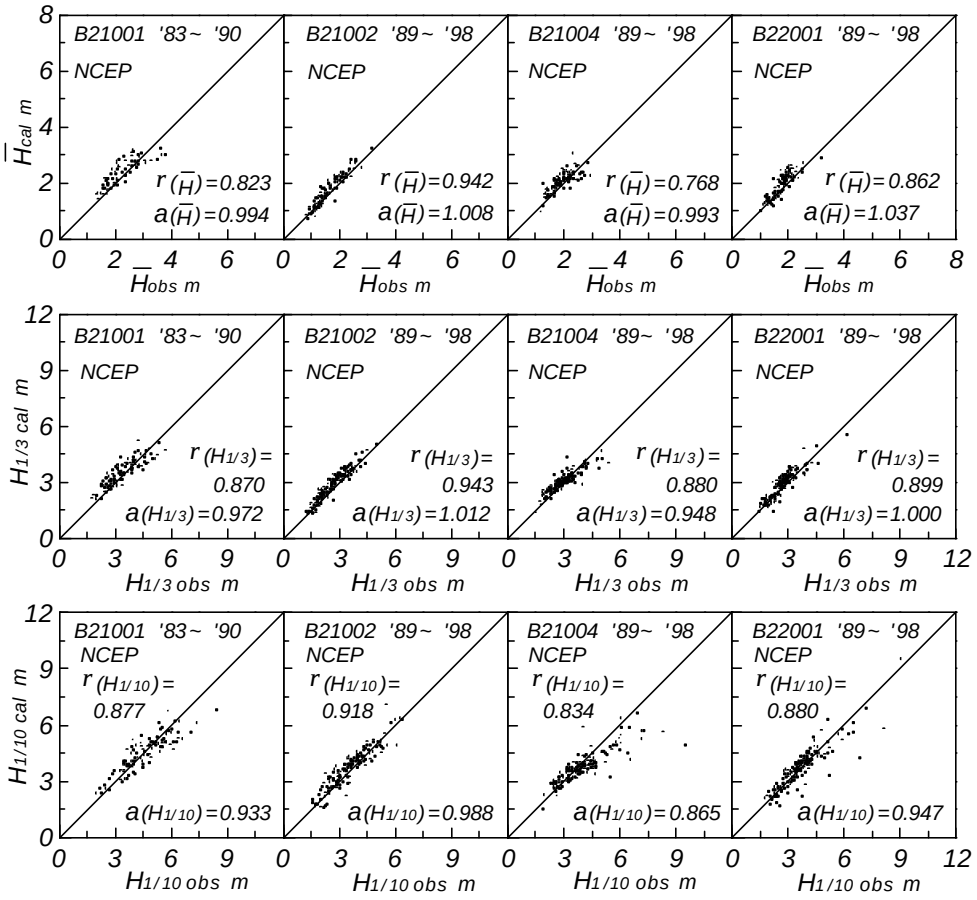

Figure 6. Comparison of monthly-grouped wave height climate parameters based on hindcast and measurement data at 4 buoy stations.

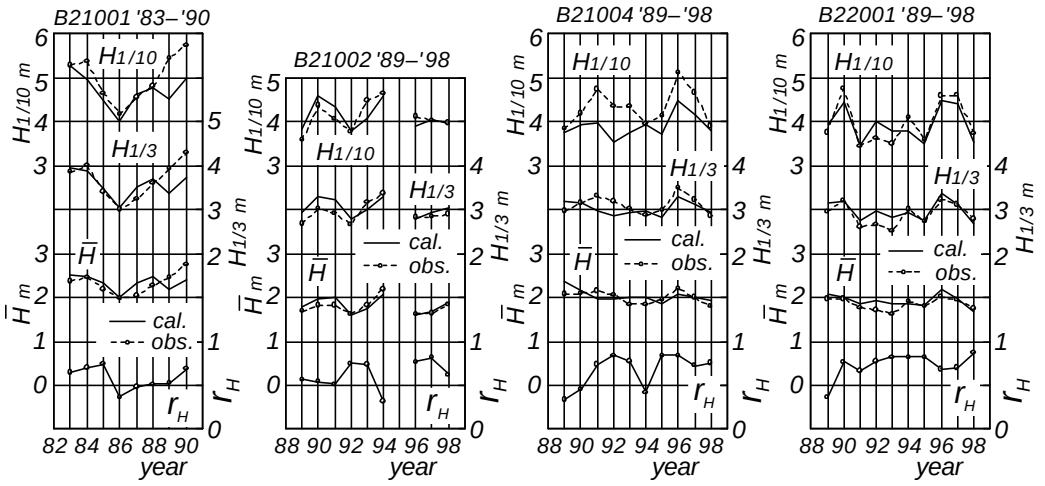

Figure 7. Comparison of yearly-grouped wave height climate parameters based on hindcast and measurement data at 4 buoy stations.

from the above discussion that $\overline{H}$ and $H_{1/3}$ rather than $H_{1/10}$ are preferable for the wave height climate parameters, when the trend of wave height is investigated using long-term wave data hindcast under the NCEP/NCAR wind conditions.

4. TREND ANALYSIS OF WINDS AND WAVES ON THE NORTHWESTERN PACIFIC OCEAN

4.1 *Long-Term Variation of Winds and Waves*

A 51-year variation of yearly-grouped climate parameters of wind speed and wave height and their deviations from overall means at B21004 is exemplified in Figure 8. The parameters and deviations are ($U_{1/3}$, ? $U_{1/3}$, $\overline{U}$, ? $\overline{U}$) for wind speed data and ($H_{1/3}$, ? $H_{1/3}$, $\overline{H}$, ? $\overline{H}$)for wave height data. Any climate parameters for both wind speed and wave height indicate an increasing trend in the first 10 years from 1948 to 1957 and subsequent small variation around a constant value from 1958 to 1998. A similar tendency is observed at the other locations. The increasing trend in the first 10 years may be due to the reanalysis wind data of poor quality in the period associated with scarcity of measurement data rather than the natural phenomenon called 'climate jump'. From the above-mentioned result, trend analysis of the climate parameters is separately conducted for the data set with the 51-year period from 1948 to 1998 and that with the 41-year period from 1958 to 1998.

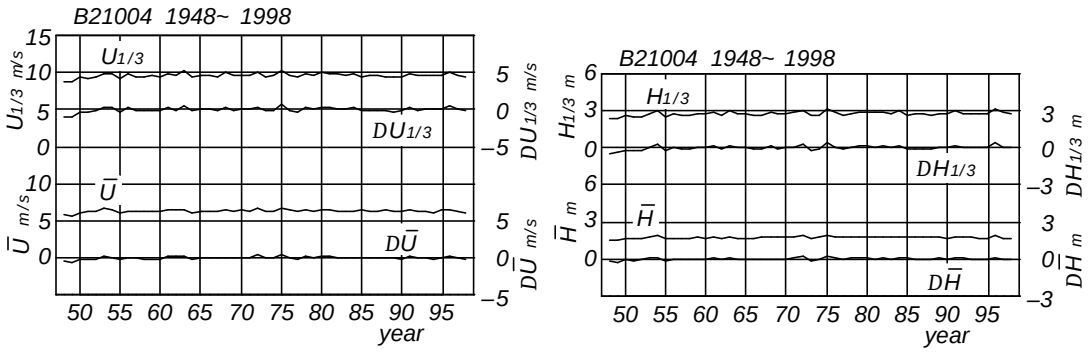

Figure 8. 51-year variation of yearly-grouped climate parameters of wind speed and wave height and their deviations from overall means at B21004.

Figure 9 shows frequency spectra for residual time series of monthly-separated $\overline{U}$ and $\overline{H}$ at B21004, in case where the Blackman-Tukey method is applied under the conditions such as time step of 1 month, sample size of 612 and lag of 48. It should be noted that the analyzed time series is made by subtracting the corresponding monthly-average over the entire period from each monthly-separated data of $\overline{U}$ or $\overline{H}$. The spectra provide the features of white noise without yielding any predominant peak. This suggests that the time series of the climate parameter for either of wind speed or wave height does not have any predominant component excluding seasonal variation with the period of 1 year.

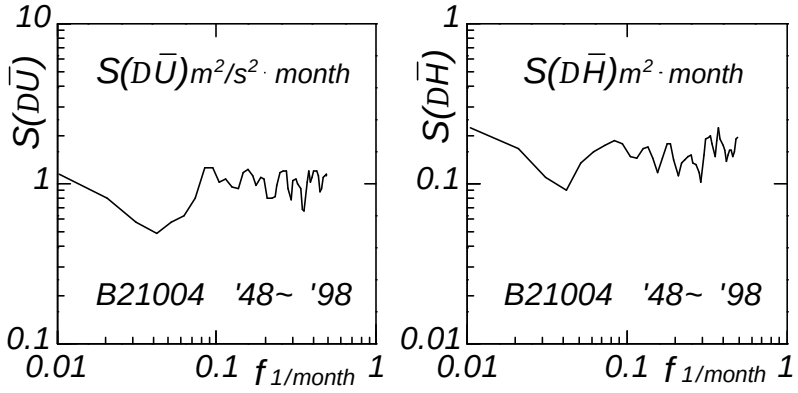

Figure 9. Spectral analyses for residual time series of monthly-grouped $U_{1/3}$ and $H_{1/3}$ at B21004.

4.2 *Trend of Winds*

Figure 10 demonstrates the slope value of a linear regression line $a(\overline{U})$ and the trend index $I_T(\overline{U})$ for yearly-separated mean wind speed data $\overline{U}$ over the Northwestern Pacific Ocean, in cases where the data periods are 51 years and 41 years. As for the 51-year period data, rough range of the slope value is between -1 and 2 cm/s/year and the value is positive except for the coastal areas of China and the southern area, increasing from the nearly central area towards the surrounding areas on the whole. The trend index shows a similar distribution to the slope value. If a limiting absolute value of the trend index $|I_T(\overline{U})|$ indicating statistical significance is roughly taken as 2, increasing or decreasing trend can be detected on several sea areas such as the northeastern and southwestern areas, corresponding to the areas with large absolute value for the slope. As for the 41-year period data, an upper bound of the slope value generally reduces to 1 cm/s/year because of elimination of the first 10 years of data in the 51-year period data which has a strong increasing rate. As a result, sea areas taking negative slope value become larger compared to those based on the 51-year period data and the areas cover the East China Sea, the Japan Sea and offshore region of the Pacific Ocean coasts of west and east Japan. The trend index suggests increasing trend with statistical significance on the southwestern area, the central area and the northeastern area and decreasing trend with statistical significance on the coastal areas of China, Russia, and west and east Japan facing the Pacific Ocean. In particular, the tendency on the northeastern area is strengthened toward the northeast direction. On the sea areas around Japan, the Japan Sea side hardly yields substantially significant trend, and the Pacific Ocean side of west and east Japan gives rise to decreasing trend. Also, weakly increasing trend is observed on the Pacific Ocean side of north Japan and on the East China Sea side of Kyushu Island located in southwest Japan.

4.3 *Trend of Waves*

A weighted linear interpolation method (Shiono et al., 1985) is applied to make the data on a 80km grid from the data at 52 irregularly-distributed points. Figure 11 shows space distributions of the mean SWH $\overline{H}$ and the highest 1/3 mean SWH $H_{1/3}$ over 41 years. The 51-year data give similar space distributions with slightly lesser values. The mean SWH $\overline{H}$ on the East China Sea and the Pacific Ocean increases from about 1 m to 2.5 m counterclockwise around Japan and that on the Japan Sea becomes larger from 1m on the southwest area towards 1.5 m on the northeast area. A similar space variation is also observed for the highest 1/3 mean SWH $H_{1/3}$ with a magnitude of 1.6 times as large as $\overline{H}$ and consequently, a small sea area with 4 m height appears on the

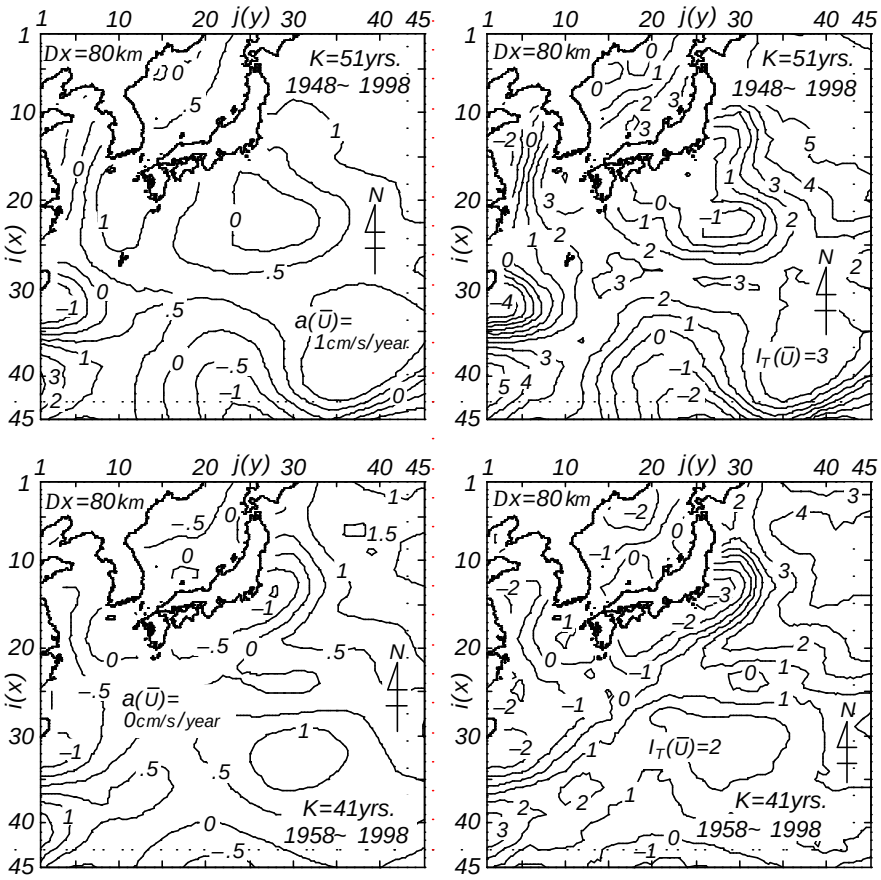

Figure 10 . Trend analysis for yearly-separated data of mean wind speed over the Northwestern Pacific Ocean.

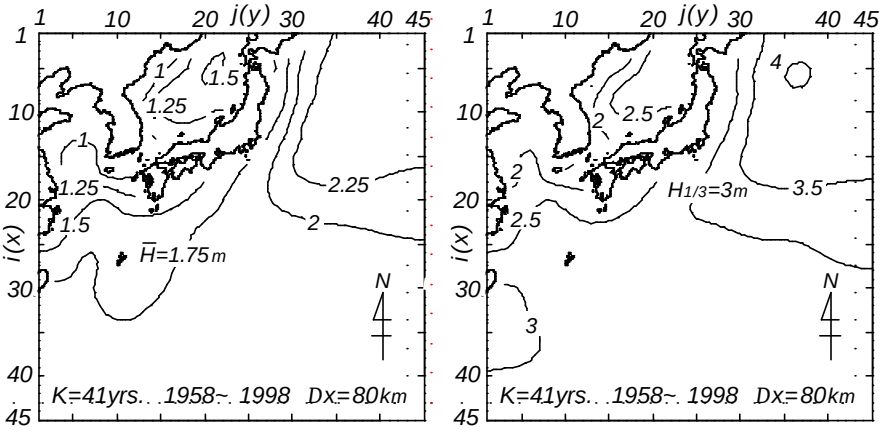

Figure 11 . Mean and highest 1/3 mean of significant wave height data over 41 years on the Northwestern Pacific Ocean.

northeastern area of the Northwestern Pacific Ocean.

Space distributions of the slope value $a(\overline{H})$ and trend index $I_T(\overline{H})$ of yearly-grouped mean SWH $\overline{H}$ are given in Figure 12 separately for the 51-year data and the 41-year data. As for the 51-year data, the slope value $a(\overline{H})$ increases from -1 mm/year on the northern area of the East China Sea to 7 mm/year on the northeast area of the Northwestern Pacific Ocean counterclockwise around Japan on the whole, in cases where the slope value from 2 to 3 mm/year covers a wide area on the western region of the Northwestern Pacific Ocean. On the Japan Sea, the slope value increases from 0 mm/year on the Russian waters to 2 mm/year on the Japanese waters towards the southeast direction. A similar distribution is obtained for the trend index, corresponding to magnitude of the slope value. A statistically significant increasing trend in cases where trend index takes a value of more than 2 in a rough sense is seen on almost all areas of the Northwestern Pacific Ocean including the southeast area of the East China Sea and the trend intensity becomes greater from the central area towards the northeast area of the Northwestern Pacific Ocean. Also, a weak but statistically significant increasing trend is observed on the Japanese waters of the Japan Sea and a decreasing trend on a small area of the Chinese waters.

As for the 41-year data, decrease of the slope value from 1 to 2 mm/year compared to that based on the 51-year data brings about enlargement of areas taking negative slope value on the East China Sea, the Japan Sea and the Northwestern Pacific Ocean area near west Japan. As a result, absolute value of trend index generally becomes smaller than 2 on the western area of the Northwestern Pacific Ocean including the East China Sea and the Japan Sea. This suggests that trend of the mean SWH $\overline{H}$ with statistical significance on the area is hardly detected except for a weakly decreasing trend on a small area of the Japan Sea. On the eastern area of the Northwestern Pacific Ocean, an increasing trend with statistical significance becomes stronger from the central area towards

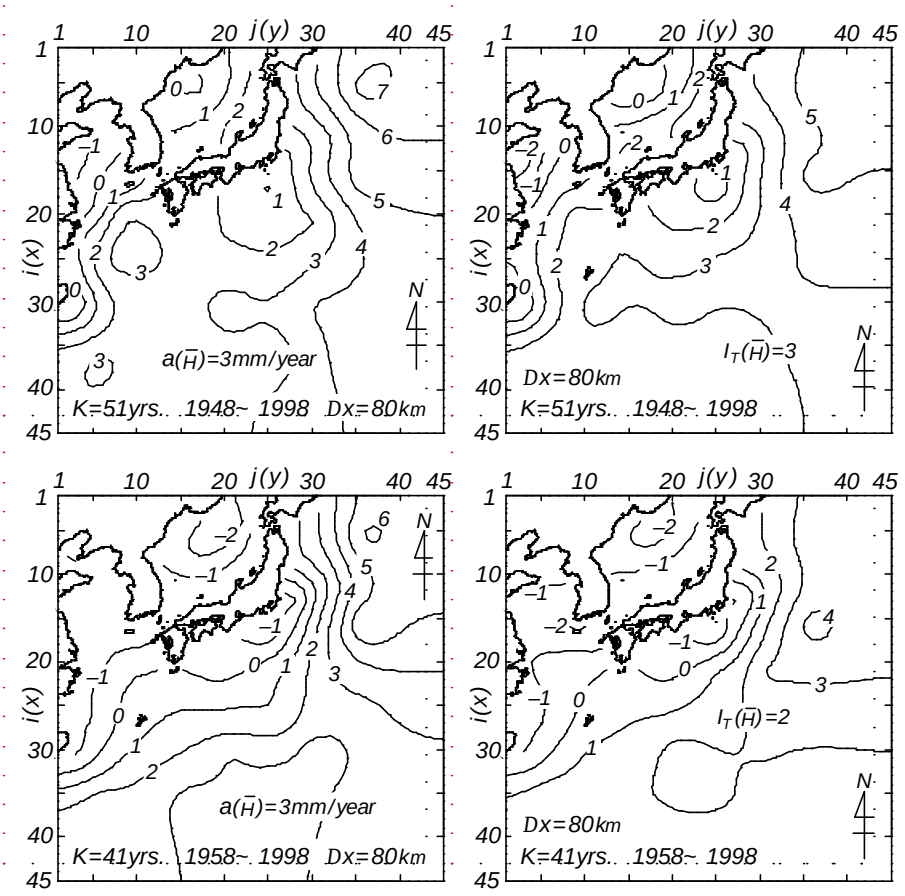

Figure 12. Trend analysis for yearly-separated data of mean significant wave height on the Northwestern Pacific Ocean.

the northeastern area. Also, a statistically significant trend is rarely observed on the coastal areas around Japan. It may be said from the slope value distribution that mean SWH $\overline{H}$ is slightly decreasing over 41 years in most of the areas.

Figure 13 illustrates trend analyses of the highest 1/3 mean SWH $H_{1/3}$ over the 41-year period on the Northwestern Pacific Ocean. Similar patterns in the cases of the mean SWH $\overline{H}$ are observed in both of the figures. But the trend intensity for $H_{1/3}$ becomes slightly weaker compared to that for $\overline{H}$, because increasing rate of the slope value $a(H_{1/3})$ to the slope value $a(\overline{H})$ is generally smaller than that of the highest 1/3 mean value $H_{1/3}$ to the mean value $\overline{H}$ on the concerned sea area. As a consequence, increasing trend of $H_{1/3}$ with statistical significance is limited on the east area of the Northwestern Pacific Ocean, which intensifies towards the northeast direction as well as in the case of $\overline{H}$.

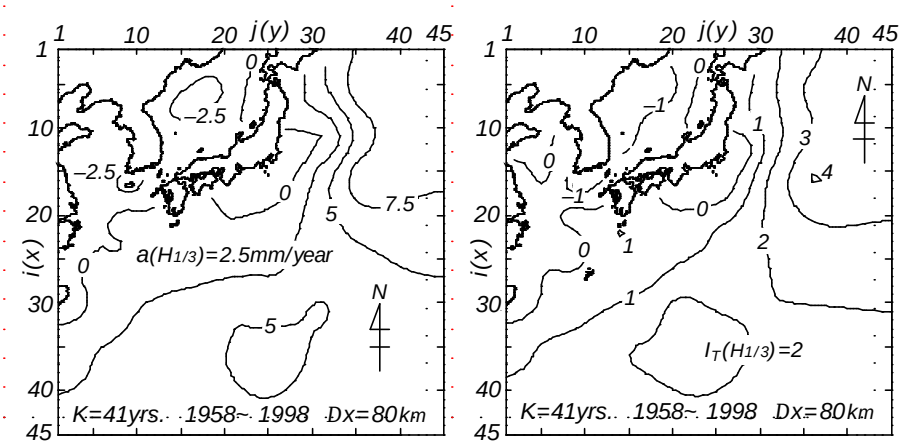

Figure 13. Trend analysis for yearly-separated data of highest 1/3 mean significant wave height on the Northwestern Pacific Ocean.

Finally, trend index for season-separated data of the mean SWH $\overline{H}$ over 41 years on the Northwestern Pacific Ocean is shown in Figure 14 for the winter season from January to March and for the summer season from July to September respectively. The overall pattern of trend index in the winter season is insignificantly different from

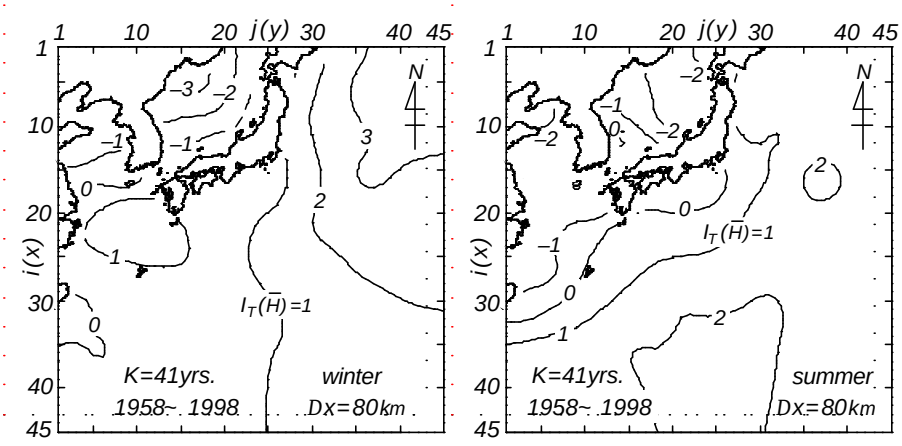

Figure 14. Trend analysis for season-separated data of mean significant wave height on the Northwestern Pacific Ocean.

that in all the seasons indicated by Figure 13, except that the decreasing trend becomes stronger on the northwestern area of the Japan Sea. In the summer season when typhoon-generated waves are usually dominant in particular on the southern sea area, an increasing trend with statistical significance tends to become weaker on the northeast area, while a weakly decreasing trend with statistical significance newly appears on the northern area of the Japan Sea.

5. CONCLUSIONS

The main results are summarized as follows;
1) The NCEP/NCAR wind data yields lower wind speed than measurement data for higher wind conditions, while it gives reasonable agreement for wind direction.
2) The backward ray tracing wave model with tuned growth term under the input conditions of NCEP/NCAR wind data reproduces satisfactorily the wave climate parameters estimated from the measurement data, although it still yields a smaller estimate for wave climate parameters representing higher wave parts in wave height data such as the highest 1/10 mean of significant wave height data.
3) A strong increasing trend of both wind and wave climate parameters on the Northwestern Pacific Ocean in the first 10 years from 1948 to 1957 is probably related to a quality problem of the NCEP/NCAR wind data.
4) Statistically significant increasing trends of both wind and wave climate parameters during the recent 41 years from 1958 to 1998 are found on the northeastern sea area of the Northwestern Pacific Ocean and the trend intensifies toward the northeast direction.
5) On the sea areas around Japan, a statistically significant increasing trend of both wind and wave climate parameters during the recent 41 years is hardly detected. Also, on the north coasts of the Japan Sea, a weakly decreasing trend of wave climate parameters is observed in the summer season when sea states are generally calm.

6. ACKNOWLEDGEMENTS

A part of this study was accomplished with the support of the Grant-in-Aid for Scientific Research (C)(2), No. 13680546 by Japan Society for the Promotion of Science, for which the authors express their appreciation. Thanks are also due to NCAR which kindly provided the NCEP/NCAR reanalysis surface wind data sets.

7. REFERENCES

Bacon, S. and D.J.T. Carter, 1991: Wave climate changes in the North Atlantic and North Sea. *Int. Jour. Climatol.*, **11**, 545-558.

Carter, D.J.T. and L. Draper, 1988: Has the northeast Atlantic become rougher?. *Nature*, **332**, 494.

Cox, A.T. and V.R. Swail, 2001: A global wave hindcast over the period 1958-1997: Validation and climate assessment. *Jour. Geophys. Res.*, **106**, **C2**, 2313- 2329.

Gunther, H. et al., 1998: The wave climate of the northeast Atlantic over the periods 1955-1994 ; The WASA wave hindcast. *Global Atmos. and Ocean System*, **6**, 121-163.

Hatada, Y., Yamaguchi, M. and H. Nonaka, 2000: One year comparison of wave hindcasts by backward ray tracing model and WAM. *Proc. 6th Int. Workshop on Wave Hindcasting and Forecasting*, 261-270.

Kushnir, T., Cardone, V.J. and J.G. Greenwood, 1997: The recent increase in North Atlantic wave heights. *Jour. Climate*, **10**, 2107-2113.

Shiono, K., Wadatsumi, K. and S. Matsumoto, 1985: A method for contouring of grid data converted from irregularly spaced data on a personal computer (1) - Weighted linear interpolation-. *Jour. Information Geology*, **10**, 65-78(in Japanese).

Sterl, L. and G.J. Komen, 1998: Fifteen years of global wave hindcasts using winds from the European Centre for Medium-Range Weather Forecasts reanalysis; Validating the reanalyzed winds and assessing the wave climate. *Jour. Geophys. Res.*, **103**, **C2**, 5477-5492.

Suzuki, E., 1975: *Meteorological Statistics*. Chijin Shokan, 314p (in Japanese).

Suzuki, Y. et al., 1996: Long-term variability of waves based on wave hindcast and buoy data. *Abstracts of Autumn Meeting by Oceanogra. Soc. of Japan in 1996*, **217**(in Japanese).

Yamaguchi, M., Hatada, Y. and Y. Utsunomiya, 1987: A shallow water wave prediction model at a single location and its applicability. *Jour. Japan Soc. for Civil Engineers*, **381/II-7**, 151-160(in Japanese).